

Supplementary information to:

**High Conductive and Metallic Cobalt-Nickel Selenide
Nanorods Supported on Ni Foam as an Efficient
Electrocatalyst for Alkaline Water Splitting**

**Shu Liu†, Yimin Jiang†, Miao Yang, Qifei Guo, Mengjie Zhang, Wei Shen,
Rongxing He*, Ming Li***

Experimental section

Materials

Nickel foam (1.0 mm thickness) was purchased from Shenzhen Green and Creative Environmental Science and Technology Co., Ltd. Pt/C catalyst (20 wt% Pt on Vulcan XC-72R carbon), RuO₂ catalyst, Nafion (5 wt%) and Se powder was obtained from Sigma-Aldrich Chemical Reagent Co., Ltd. Other chemicals were of analytical grade and used without further purification. The water used throughout all experiments was purified through a Millipore system.

Synthesis of Co-based/NF precursor

Prior to the synthesis, the nickel foam (NF) was ultrasonicated with acetone, 3.0M HCl aqueous solution, absolutely ethanol and deionized water for 10 min, respectively, and then dried in a vacuum oven at room temperature. Co-based/NF precursor was synthesized via a hydrothermal process. In a typical synthesis,¹ 1mmol Co(CH₃COO)₂·4H₂O, 2.5mmol NH₄F, and 5mmol urea was dissolved into 15 mL of deionized water. The obtained pink solution was transferred into 25 mL Teflon-lined autoclave with a piece of pre-treated Ni foam (1x3 cm). Then the autoclave was heated and maintained at 120 °C for 6 h. After it was cooled down naturally to room temperature, the sample was washed with distilled water and ethanol several time, and dried in a vacuum oven for 6 h. The annealed precursor was synthesized by an annealing treatment in N₂ environment at 350 °C with a ramping rate of 2 °C min⁻¹ for 2h.

Synthesis of Co_{0.75}Ni_{0.25}Se/NF and NiSe/NF

Se powder (0.059 g) was added into deionized water (1.5 mL) containing NaBH₄

(0.065 g). After gentle stirring for 30 min, a clear NaHSe solution was obtained. The freshly prepared NaHSe solution was added into a mixed solution included 3 mL ethanediamine (EDA) and 22 mL ethanol (ET) under N₂ flow. Then the solution was transferred into 50 mL Teflon-lined autoclave with a piece of Co-based/NF precursor and maintained at 160 °C for 10 h. After it was cooled down naturally to room temperature, the sample was washed with distilled water and ethanol several time, and then dried at room temperature. The NiSe/NF was prepared from bare nickel foam under the same conditions used for preparing Co_{0.75}Ni_{0.25}Se/NF.

Preparation of Pt/C and RuO₂ electrode:

10 mg commercial Pt/C (20 wt.%) or RuO₂ and 50 μL Nafion solution (5 wt.%) were dispersed in water/ethanol solvent (500 μL distilled water and 450 μL ethanol) by 30 min sonication to form an ink. Then 200 μL catalyst ink was uniformly drop-cast onto the 1x1 cm Ni foam and air-dried at room temperature.

Physical Characterizations:

XRD data were measured on a RigakuD/MAX 2550 diffractometer with Cu K α radiation ($\lambda=1.5418$ Å). SEM measurements were acquired using a XL30 ESEM FEG scanning electron microscope at an accelerating voltage of 20 kV. TEM and HRTEM images were collected using a TF20. XPS was performed on an ESCALAB 250XI spectrometer with a mono X-ray source Al k α excitation. Surface areas were calculated by Brunauer-Emmett-Teller (BET) method. Element content was determined by an inductively coupled plasma-atomic emission spectrometer (ICP-AES, PE2100DV).

Electrochemical measurements:

Electrochemical measurements were performed with a CHI 660E electrochemical analyzer (CH Instruments, Inc., Shanghai) in a standard three-electrode system in 1 M KOH, with the use of a graphite rod and a saturated calomel electrode (SCE) as the counter and the reference electrode, respectively. In all measurements, the SCE reference electrode was changed to E(RHE) according to the formula $E(\text{RHE}) = E(\text{SCE}) + 0.242 + 0.05916 \times \text{pH}$. The synthesized samples were used as working electrodes. The linear sweep voltammetry measurements were conducted with a scan rate of 5 mV s^{-1} for HER and 1 mV s^{-1} for OER. The electrochemical impedance spectroscopy (EIS) was carried out at an overpotential of 120 mV for HER and 300 mV for OER in a frequency range from 100 kHz to 10 mHz. Chronopotentiometric measurements were carried out at an overpotential of 120 mV for HER and 250 mV for OER. All plots for evaluating the electrocatalytic activity toward the HER and OER were corrected by an ohmic potential drop (iR) based on the series resistances derived from EIS. For comparison, the electrocatalytic activities of other samples were also measured under the similar condition.

Turnover frequency (TOF) calculations:

The number of active sites (n) was determined using a previously reported method^{2, 3} by (CV) curves collected from -0.2 to +0.6 V vs. RHE in phosphate buffered saline solution (PBS, pH = 7.0) with a scan rate of 0.05 V s^{-1} . While it is difficult to assign the observed peaks to a given redox couple, n should be proportional to the integrated charge over the whole potential range. Assuming a one electron process for both

reduction and oxidation, the upper limit of n could be calculated according to the formula:

$$n(\text{mol}) = \frac{Q}{2F}$$

TOF can be calculated according to the formula:

$$TOF = \frac{J}{mFn}$$

where Q is the voltammetric charge capacity obtained by integrating the CV curves, F is the Faradic constant (96485 C mol^{-1}), J is the current density (A) during the linear sweep measurement, and the factor of $1/m$ arrives by taking into account that m electrons are consumed to form one H_2 or O_2 molecule from water (2 electrons for HER and 4 electrons for OER).

Calculation method

The electronic properties of electrocatalysts were performed using density functional theory (DFT) calculation with the program package of DMol3 package in materials studio. GGA with PBE functional was used for exchange correlation energy, and the double numerical plus polarization function (DNP) basis set were adopted. DFT semi-core pseudopotential (DSPPs) method was used for the core treatment of metal atoms. The self-consistent field (SCF) tolerance was $1 \times 10^{-5} \text{ eV}$. The K-point set was $5 \times 5 \times 1$. Combining the XRD and HRTEM dates, the (101) facet was modeled for calculation of adsorption energy. We adopted slabs with two layers for NiSe/CoSe, which includes 64 atoms ($\text{Ni}_{32}\text{Se}_{32}/\text{Co}_{32}\text{Se}_{32}$). To avoid interaction between the neighboring images, the vacuum in the direction perpendicular to the surface was set to be 15 \AA .⁴ Furthermore, the $\text{Co}_{28}\text{Ni}_4\text{Se}_{32}$ was built by substituting four Ni atoms for

four Co atoms from $\text{Co}_{32}\text{Se}_{32}$. The Gibbs free-energy (ΔG_{H^*}) is expressed as: ^{5, 6}

$$\Delta G_{\text{H}^*} = \Delta E_{\text{H}^*} + \Delta E_{\text{ZPE}} - T\Delta S$$

Where ΔE_{H^*} is the adsorption energy of hydrogen species on the catalyst surface, ΔE_{ZPE} is the zero-point energy change between the adsorbed hydrogen and hydrogen in the gas phase and ΔS is entropy change of H^* adsorption. Due to the entropy of hydrogen in adsorbed state is negligible, ΔS can be calculated as $-1/2 S_0$, among which S_0 is the entropy of H_2 in the gas phase at standard conditions and 1 bar of H_2 and $\text{pH}=0$ at 300 K. Therefore the free energy of the adsorbed state can be taken as:⁷

$$\Delta G_{\text{H}^*} = \Delta E_{\text{H}^*} + 0.24 \text{ eV}$$

HER active sites for electrocatalysts were performed by adding a hydrogen atom on the electrocatalysts surface. Pt was selected as standard electrode for free energy calculation.

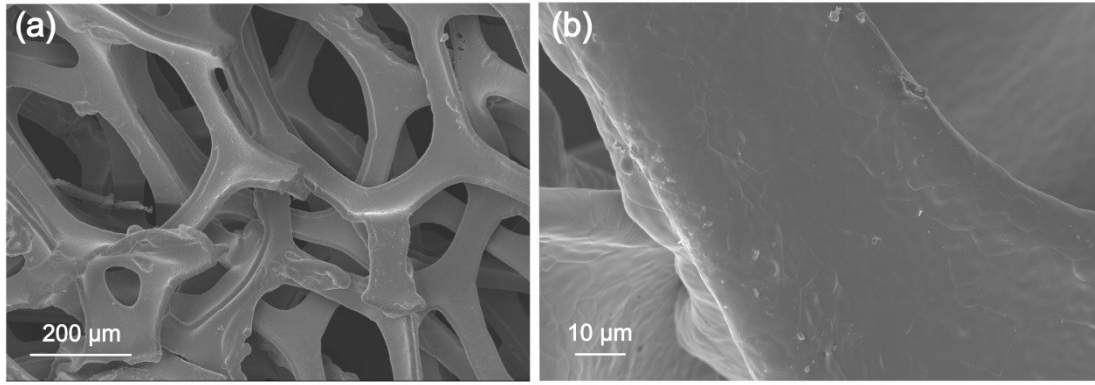


Figure S1. The SEM images of pristine Ni foam at different magnifications.

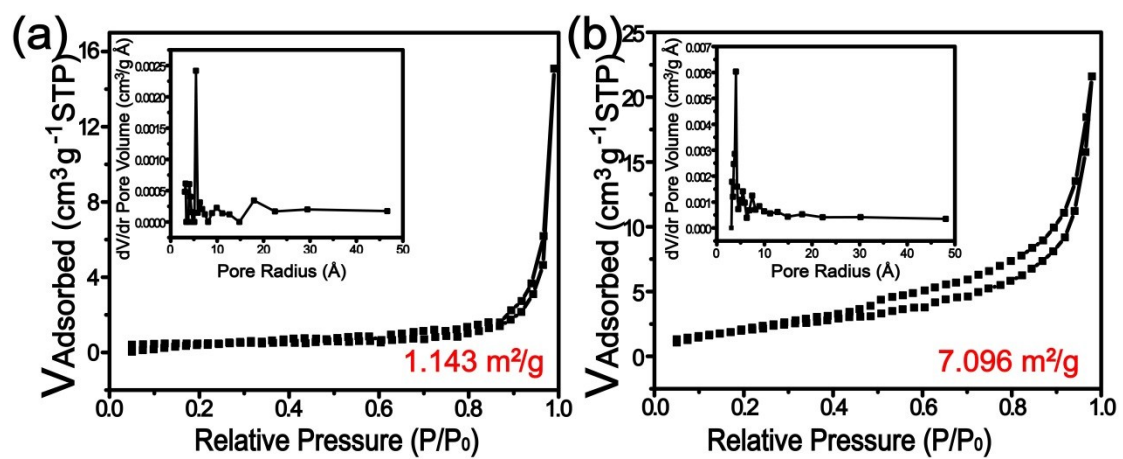


Figure S2. N_2 sorption-desorption isotherms and pore size distributions of Co-based/NF precursor (a) and $\text{Co}_{0.75}\text{Ni}_{0.25}\text{Se}/\text{NF}$ (b).

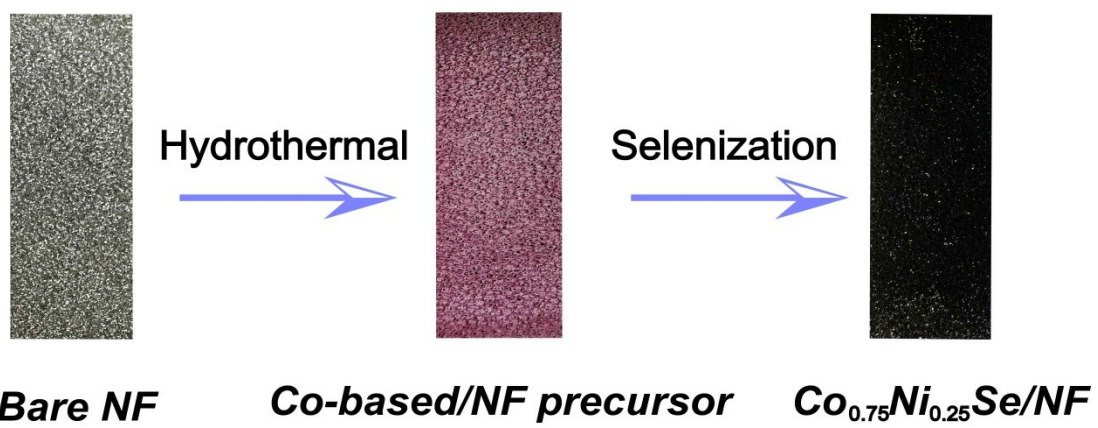


Figure S3. Optical images of pristine Ni foam, Co-based/NF precursor and $\text{Co}_{0.75}\text{Ni}_{0.25}\text{Se/NF}$

Table S1. XPS atomic ratio for the $\text{Co}_{0.75}\text{Ni}_{0.25}\text{Se/NF}$

Elem.	Co	Ni	Se	C
At.%	13.27	4.71	15.94	66.08

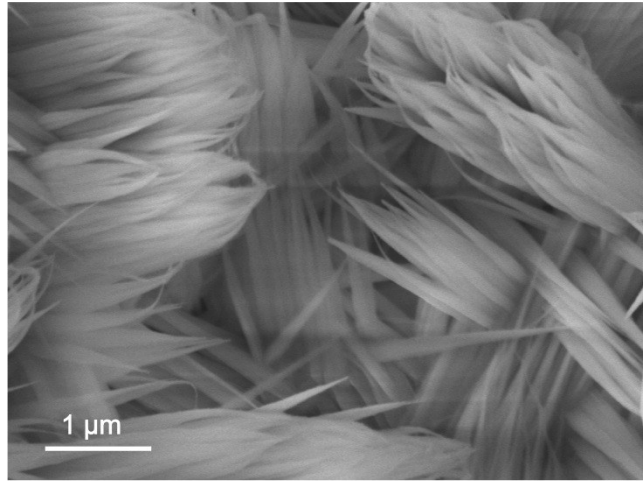


Figure S4. The SEM images of Co-based/NF precursor.

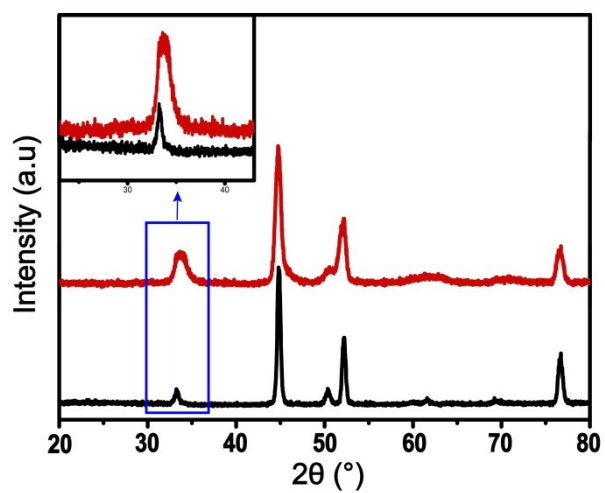


Figure S5. XRD pattern of $\text{Co}_{0.75}\text{Ni}_{0.25}\text{Se/NF}$ (red) and NiSe/NF (black)

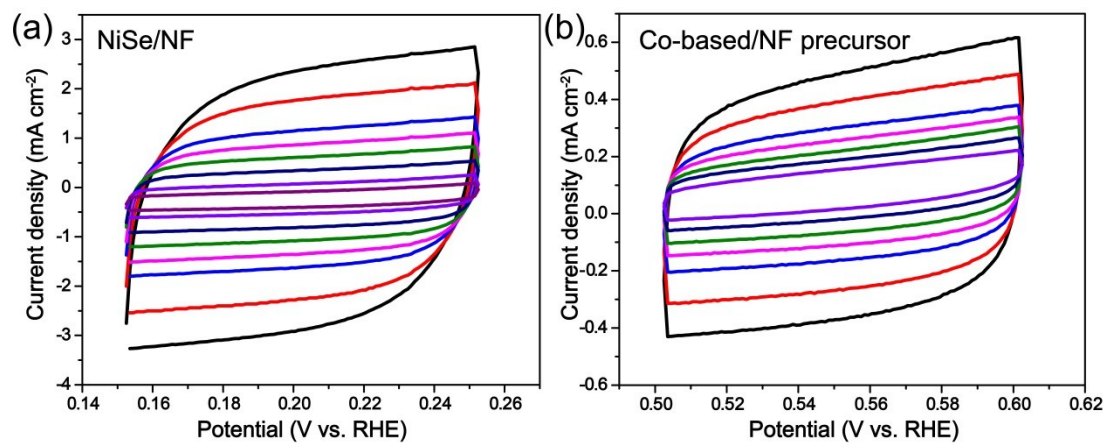


Figure S6. CVs of NiSe /NF (a) and Co-based precursor (b) at scan rates from 10, 20, 40, 60, 80, 100, and 150 to 200mV s⁻¹.

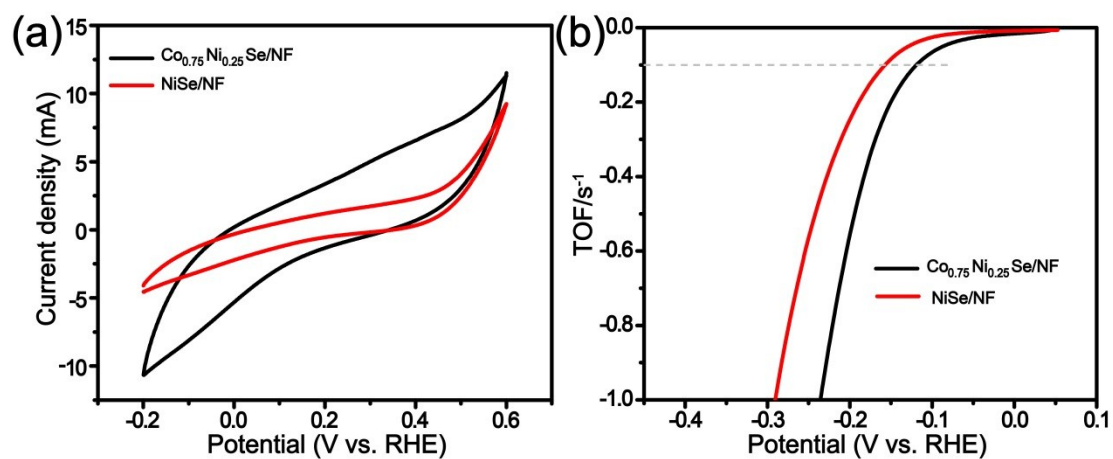


Figure S7. (a) CVs of NiSe/NF and $\text{Co}_{0.75}\text{Ni}_{0.25}\text{Se/NF}$ recorded in phosphate buffer solution with pH 7.0 at a scan rate of 50 mV s^{-1} . (b) LSV curves normalized by the active sites and expressed in the form of TOF of corresponding catalysts.

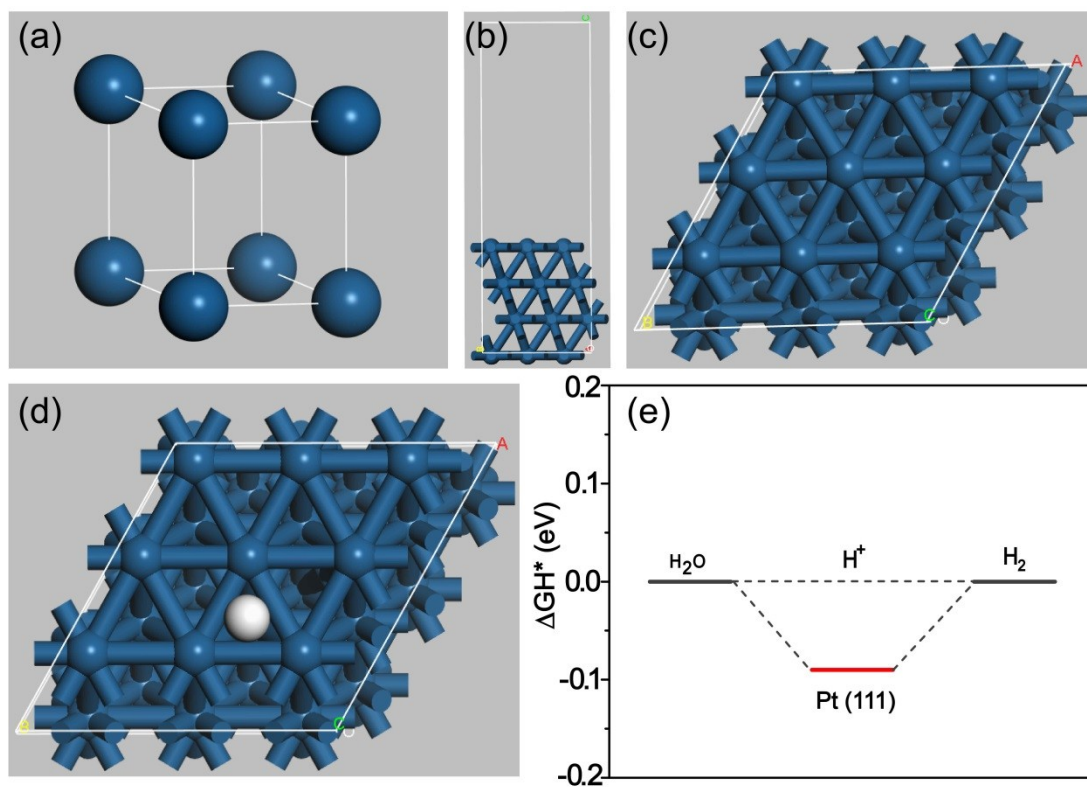


Figure S8. (a) Atomic structure model of Pt. Schematic models of Pt (111) slabs (b): side view, c: top view). (d) HER free-energy for the Pt (111).

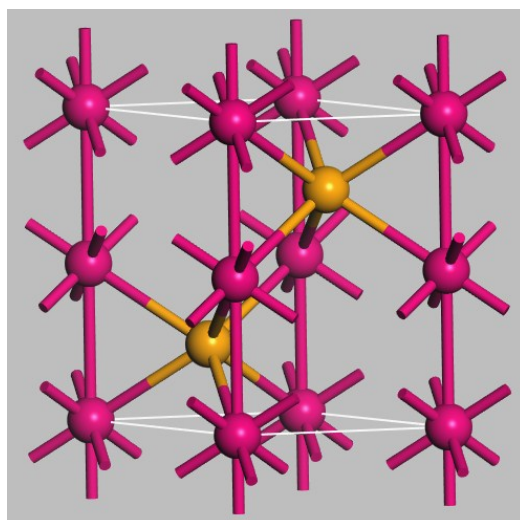


Figure S9. Atomic structure model of NiSe

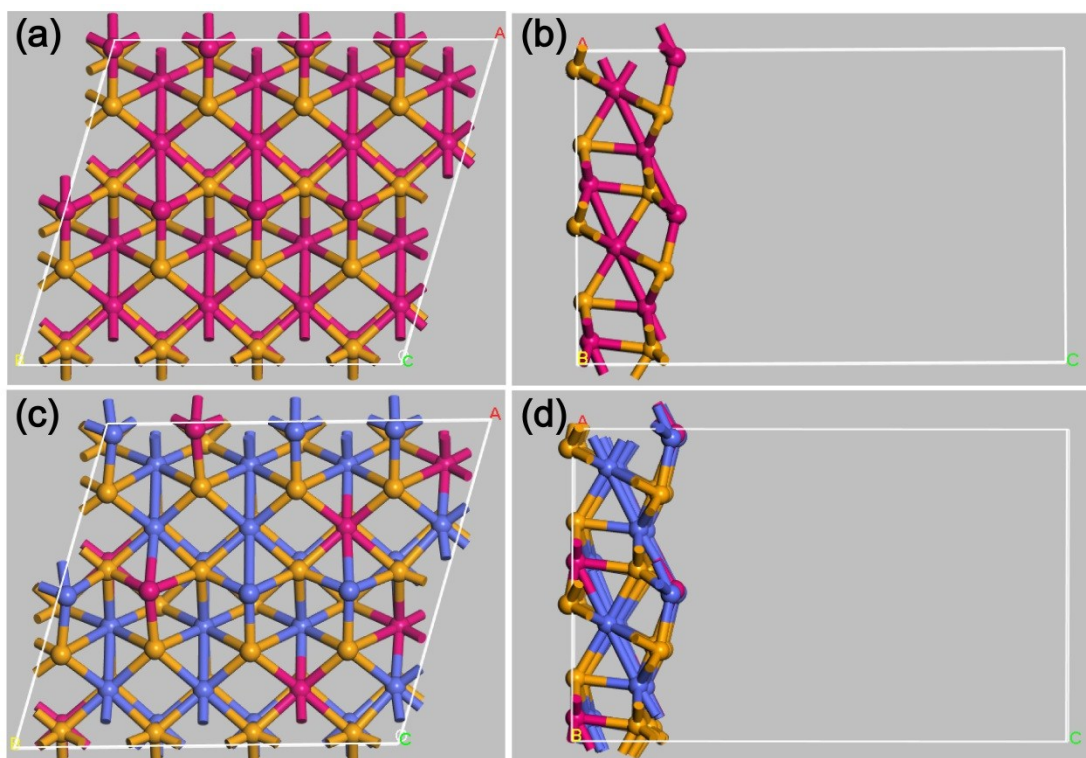


Figure S10. Schematic models of $\text{Ni}_{32}\text{Se}_{32}$ slabs (a: top view, b: side view) and $\text{Co}_{24}\text{Ni}_8\text{Se}_{32}$ (c: top view, d: side view).

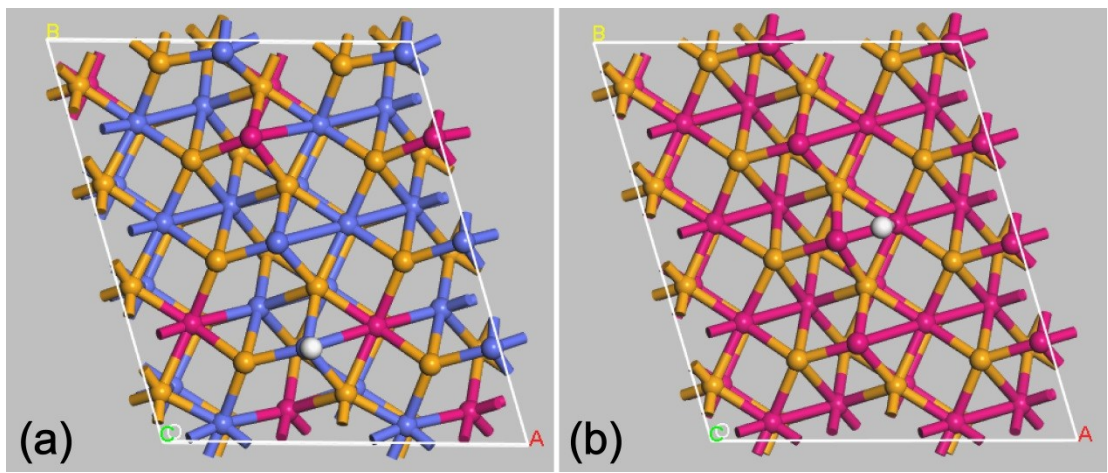


Figure S11. Top-view schematic models of $\text{Co}_{24}\text{Ni}_8\text{Se}_{32}$ and $\text{Ni}_{32}\text{Se}_{32}$ with H proton absorbed on its surface.

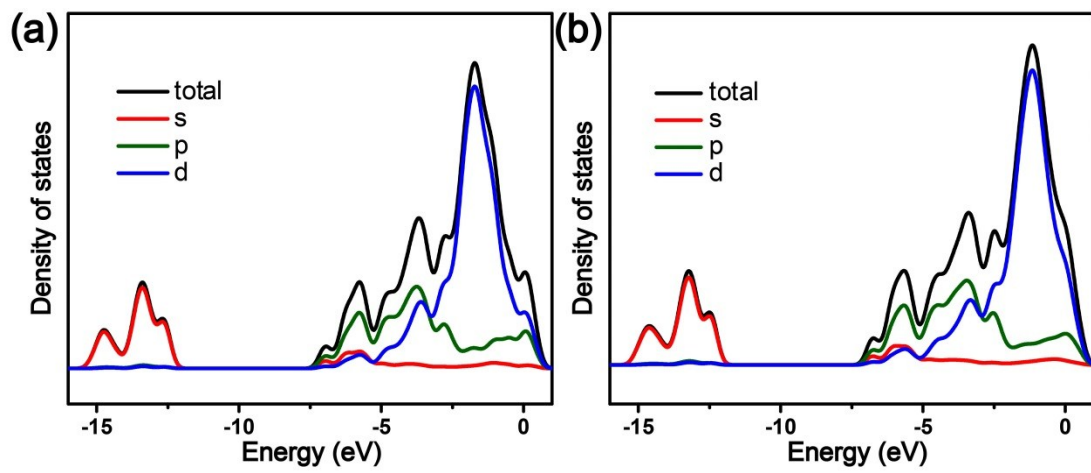


Figure S12. The density of states (DOS) spectra of as-obtained (a) NiSe and (b)

Co_{0.75}Ni_{0.25}Se

Table S2. Comparison of the electrocatalytic performance of $\text{Co}_{0.75}\text{Ni}_{0.25}\text{Se}/\text{NF}$ with Co-based electrocatalysts reported recently for OER

Catalyst	Overpotential	Substrate	Reference
$\text{Co}_{0.75}\text{Ni}_{0.25}\text{Se}/\text{NF}$	269 (50 mA cm ⁻²) 293 (100 mA cm ⁻²)	Ni foam	This work
NiFe LDH/NiCo ₂ O ₄ /NF	290 (50 mA cm ⁻²)	Ni foam	8
Co ₂ P/Co-foil	319 (10 mA cm ⁻²)	Co foil	9
Co(S _{0.22} Se _{0.78}) ₂	283 (10 mA cm ⁻²)	Glassy carbon	10
NiMoP ₂	320 (10 mA cm ⁻²) 400 (100 mA cm ⁻²)	Carbon cloth	11
(Ni,Co) _{0.85} Se NSAs	287 (20 mA cm ⁻²)	Ni foam	12
NiSe-Ni _{0.85} Se/CP	300 (10 mA cm ⁻²)	Carbon paper	13
O-CoMoS	272 (10 mA cm ⁻²)	Carbon fiber	14
a-CoSe/Ti mesh	292 (10 mA cm ⁻²)	Ti mesh	15
MOF-derived CoSe ₂	330 (10 mA cm ⁻²)	Glassy carbon	16
Mn-Co-Se	243 (10 mA cm ⁻²)	Ni foam	17
Two-tiered NiSe	290 (10 mA cm ⁻²)	Ni foam	18
NF@NC-CoFe ₂ O ₄ /C NRAs	240 (10 mA cm ⁻²)	Ni foam	19
A-CoS _{4.6} O _{0.6} PNCs	290 (10 mA cm ⁻²)	Glassy carbon	20
Ni-Fe disulfide@oxyhydroxide	230 (10 mA cm ⁻²)	Glassy carbon	21
MoS ₂ -Ni ₃ S ₂ HNRs/NF	249 (10 mA cm ⁻²)	Ni foam	22
CoO _x -CoSe	300 (100 mA cm ⁻²)	Ni foam	23

Table S3. Comparison of the electrocatalytic performance of $\text{Co}_{0.75}\text{Ni}_{0.25}\text{Se}/\text{NF}$ with Co-based electrocatalysts reported recently for HER

Catalyst	Overpotential (10 mA cm ⁻²)	Substrate	Reference
$\text{Co}_{0.75}\text{Ni}_{0.25}\text{Se}/\text{NF}$	106 mV	Ni foam	This work
NF- $\text{Ni}_3\text{S}_2/\text{NF}$	135 mV	Ni foam	3
FeNiOH/NF	160 mV	Ni foam	24
Ni-Co-P/NF	156 mV	Ni foam	25
Co- $\text{Ni}_3\text{S}_2@\text{CNT}/\text{GNF}$	155 mV	Graphite foam	26
$\text{Ni}_{4.3}\text{Co}_{4.7}\text{S}_8$	148 mV	Ni foam	27
NiS- $\text{Ni}_9\text{S}_8\text{-NiSe-NR}/\text{NF}$	112 mV	Ni foam	28
$(\text{Ni},\text{Co})_{0.85}\text{Se NSAs}$	169 mV	Ni foam	12
$\text{CoNi}_2\text{Se}_4@\text{Au}/\text{glass}$	220 mV	Glassy carbon	29
$\text{MoSe}_2@\text{Ni}_{0.85}\text{Se}$	117 mV	Ni foam	30
a-CoSe/Ti mesh	121 mV	Ti mesh	15
$\text{Co}_2\text{P}/\text{Co-foil}$	157 mV	Co foil	9
$\text{Co}(\text{S}_{0.22}\text{Se}_{0.78})_2$	122 mV	Glassy carbon	10

Table S4. Comparison of the electrocatalytic performance of $\text{Co}_{0.75}\text{Ni}_{0.25}\text{Se}/\text{NF}$ with Co-based electrocatalysts reported recently for overall water splitting

Catalyst	Overpotential (10 mA cm ⁻²)	Substrate	Reference
$\text{Co}_{0.75}\text{Ni}_{0.25}\text{Se}/\text{NF}$	1.60 V	Ni foam	This work
NiFe LDH/ $\text{NiCo}_2\text{O}_4/\text{NF}$	1.60 V	Ni foam	8
$\text{Co}_2\text{P}/\text{Co}$ -foil	1.71 V	Co foil	9
$\text{Co}(\text{S}_{0.22}\text{Se}_{0.78})_2$	1.63 V	Ni foam	10
NiMoP_2	1.65 V	Carbon cloth	11
$\text{NiCo}_2\text{S}_4@\text{NiFe}$ LDH	1.60 V	Ni foam	31
$(\text{Ni},\text{Co})_{0.85}\text{Se}$ NSAs	1.65 V	Ni foam	12
$\text{NiSe}-\text{Ni}_{0.85}\text{Se}/\text{CP}$	1.62 V	Carbon paper	13
O-CoMoS	1.6 V	Carbon fiber	14
a-CoSe/Ti mesh	1.65 V	Ti mesh	15
CoO_x-CoSe	~1.64 V	Ni foam	23

References

1. Q. Liu, J. Shi, J. Hu, A. M. Asiri, Y. Luo and X. Sun, *ACS Appl. Mater. Interfaces*, 2015, **7**, 3877-3881.
2. Y. Pan, Y. Chen, Y. Lin, P. Cui, K. Sun, Y. Liu and C. Liu, *J. Mater. Chem. A*, 2016, **4**, 14675-14686.
3. L. Zeng, K. Sun, Z. Yang, S. Xie, Y. Chen, Z. Liu, Y. Liu, J. Zhao, Y. Liu and C. Liu, *J. Mater. Chem. A*, 2018, **6**, 4485-4493.
4. Z. L. Wang, *J. Phys. Chem. B*, 2000, **104**, 1153-1175.
5. J. K. Norskov, T. Bligaard, A. Logadottir, J. R. Kitchin, J. G. Chen, S. Pandalov and J. K. Norskov, *J. Electrochem. Soc*, 2005, **152**, J23-J26.
6. W. Sheng, M. Myint, J. G. Chen and Y. Yan, *Energy Environ. Sci*, 2013, **6**, 1509-1512.
7. Y. Zheng, Y. Jiao, Y. Zhu, L. H. Li, Y. Han, Y. Chen, A. Du, M. Jaroniec and S. Z. Qiao, *Nat. Commun.*, 2014, **5**, 3783.
8. Z. Wang, S. Zeng, W. Liu, X. Wang, Q. Li, Z. Zhao and F. Geng, *ACS Appl. Mater. Interfaces*, 2017, **9**, 1488-1495.
9. C.-Z. Yuan, S.-L. Zhong, Y.-F. Jiang, Z. K. Yang, Z.-W. Zhao, S.-J. Zhao, N. Jiang and A.-W. Xu, *J. Mater. Chem. A*, 2017, **5**, 10561-10566.
10. L. Fang, W. Li, Y. Guan, Y. Feng, H. Zhang, S. Wang and Y. Wang, *Adv. Funct. Mater.*, 2017, **27**, 1701008.
11. X.-D. Wang, H.-Y. Chen, Y.-F. Xu, J.-F. Liao, B.-X. Chen, H.-S. Rao, D.-B. Kuang and C.-Y. Su, *J. Mater. Chem. A*, 2017, **5**, 7191-7199.
12. K. Xiao, L. Zhou, M. Shao and M. Wei, *J. Mater. Chem. A*, 2018, **6**, 7585-7591.
13. Y. Chen, Z. Ren, H. Fu, X. Zhang, G. Tian and H. Fu, *Small*, 2018, **14**, 1800763.
14. J. Hou, B. Zhang, Z. Li, S. Cao, Y. Sun, Y. Wu, Z. Gao and L. Sun, *ACS Catal.*, 2018, **8**, 4612-4621.
15. T. Liu, Q. Liu, A. M. Asiri, Y. Luo and X. Sun, *Chem. Commun.*, 2015, **51**, 16683-16686.
16. X. Liu, Y. Liu and L.-Z. Fan, *J. Mater. Chem. A*, 2017, **5**, 15310-15314.
17. G. Mei, H. Liang, B. Wei, H. Shi, F. Ming, X. Xu and Z. Wang, *Electrochim. Acta*, 2018, **290**, 82-89.
18. H. Wu, X. Lu, G. Zheng and G. W. Ho, *Adv. Energy Mater.*, 2018, **8**, 1702704.
19. X. F. Lu, L. F. Gu, J. W. Wang, J. X. Wu, P. Q. Liao and G. R. Li, *Adv. Mater.*, 2017, **29**, 1604437.
20. P. Cai, J. Huang, J. Chen and Z. Wen, *Angew. Chem., Int. Ed.*, 2017, **56**, 4858-4861.
21. M. Zhou, Q. Weng, X. Zhang, X. Wang, Y. Xue, X. Zeng, Y. Bando and D. Golberg, *J. Mater. Chem. A*, 2017, **5**, 4335-4342.
22. Y. Yang, K. Zhang, H. Ling, X. Li, H. C. Chan, L. Yang and Q. Gao, *ACS Catal.*, 2017, **7**, 2357-2366.
23. X. Xu, P. Du, Z. Chen and M. Huang, *J. Mater. Chem. A*, 2016, **4**, 10933-10939.
24. J. T. Ren, G. G. Yuan, C. C. Weng, L. Chen and Z. Y. Yuan, *Nanoscale*, 2018, **10**, 10620-10628.
25. Y. Gong, Z. Xu, H. Pan, Y. Lin, Z. Yang and J. Wang, *J. Mater. Chem. A*, 2018, **6**, 12506-12514.
26. F. Wang, Y. Zhu, W. Tian, X. Lv, H. Zhang, Z. Hu, Y. Zhang, J. Ji and W. Jiang, *J. Mater. Chem. A*, 2018, **6**, 10490-10496.
27. Y. Tang, H. Yang, J. Sun, M. Xia, W. Guo, L. Yu, J. Yan, J. Zheng, L. Chang and F. Gao, *Nanoscale*, 2018, **10**, 10459-10466.
28. H. Meng, W. Zhang, Z. Ma, F. Zhang, B. Tang, J. Li and X. Wang, *ACS Appl. Mater. Interfaces*,

2018, **10**, 2430-2441.

29. B. G. Amin, A. T. Swesi, J. Masud and M. Nath, *Chem. Commun.*, 2017, **53**, 5412-5415.
30. C. Wang, P. Zhang, J. Lei, W. Dong and J. Wang, *Electrochim. Acta*, 2017, **246**, 712-719.
31. J. Liu, J. Wang, B. Zhang, Y. Ruan, L. Lv, X. Ji, K. Xu, L. Miao and J. Jiang, *ACS Appl. Mater. Interfaces*, 2017, **9**, 15364-15372.